Fermi National Accelerator Laboratory

FERMILAB-Pub-90/176-A
August 22, 1990

P-22

Microwave Background Distortions from Domain Walls

GUENTER GOETZ

DIRK NÖTZOLD*

Astronomy and Astrophysics Center,

University of Chicago, Chicago IL 60637

and

NASA/Fermilab Astrophysics Center, Fermi

National Accelerator Laboratory, Batavia, IL 60510.

ABSTRACT

Domain walls arising in a cosmic phase transition after decoupling were recently proposed as seeds for the formation of large scale structure. The distortion induced in the microwave background radiation is calculated in dependence of the wall thickness, surface density, scalar field potential, cosmic redshift and the velocity of the wall. We find that the maximal redshift distortion for both spherical and planar walls is of the order $\pi G\sigma H_0^{-1}$, where σ is the surface energy density and H_0^{-1} the Hubble parameter. We also find that, for a wall thickness smaller than the horizon, walls can be treated as infinitely thin, i.e. the redshift distortion is independent of the wall thickness and the specific form of the scalar potential. For planar walls moving with a Lorentz-factor γ the redshift distortion is enhanced by γ^3.

* address after Sept. 15, 1990: CBPF, Rio de Janeiro, Brazil, bitnet: Dirc @ LNCC

1. Introduction

As a product of a phase transition in the universe domain walls, like other topological defects as strings, monopols and textures, can play an important role in the process of structure formation. Domain walls produced during a GUT phase transition were shown to have disastrous consequences because their energy density would soon have dominated the matter content of the universe[1]. However, recently Hill, Schramm and Fry[2] proposed a new scenario of structure formation in which light domain walls created after recombination, could seed galaxies without leading to such unacceptable consequences as the GUT wall scenario. Also, since the domain walls are formed after recombination it is expected that the induced fluctuations in the microwave background are smaller than in the previously proposed scenarios.

The dynamics of a network of domain walls was simulated numerically in Ref. 3. It was found there that closed domain walls smaller than the horizon (vacuum bubbles) collapse with almost the speed of light and only domain walls larger than the Hubble-scale are stable. The collapsing vacuum bubbles quickly become spherical due to their surface tension. The bubbles larger than the horizon, for the sake of simplicity, will here be approximated as infinite planes. In previous estimates[2] the redshift distortion for those two types of domain walls were $\delta E/E \approx G\sigma R$ where R is the thickness of the wall for bubbles or the horizon scale for planar walls.

In this paper we present a detailed calculation of the redshift distortion induced by domain walls in dependence of the wall thickness, surface density, scalar field potential, cosmic redshift and the velocity of the walls. We find that the maximal redshift distortion for both types of domain walls is of the order $\pi G\sigma H_0^{-1}$, where H_0 is the Hubble parameter, which is larger than was generally expected. Comparing this redshift distortion with the current upper limit on the anisotropy of the microwave background yields an upper limit on σ of $\sigma \lesssim 1$ MeV^3, which can still be met by the models proposed in Ref. 2.

In section 2 we give the general formula for the redshift distortion induced by the metric perturbations of domain walls in an expanding universe. This formula is evaluated for planar domain walls in section 3 and for spherical bubbles in section 4. In section 3 we analyze the dependence of the redshift distortion on the wall thickness, the scalar field potential, the cosmic redshift, the surface energy density and the velocity of the walls.

2. Redshift formula

In this paragraph we set up the formalism,to evaluate the redshift distortions caused by domain walls. The domain walls perturb the Friedman-Robertson-Walker (FRW) metric and therefore lead to distortions in the redshift of photons. The flat background FRW metric in conformal coordinates is $g_{\mu\nu} = a^2(t)\eta_{\mu\nu}$ where $\eta_{\mu\nu} = \mathrm{diag}(1,-1,-1,-1)$ with $a(t) = a(t_0)t^2/t_0^2$, since we are interested in the epoch after recombination where the universe is matter dominated. The domain walls lead to perturbations $h_{\mu\nu} \ll 1$ of this background metric so that the total metric becomes $g_{\mu\nu} = a^2(t)(\eta_{\mu\nu}+h_{\mu\nu})$. To obtain the redshift distortion caused by the metric perturbations, one has to calculate the redshift of photons in the perturbed metric $g_{\mu\nu}$ and compare it with the usual redshift relation in an unperturbed FRW-universe.

We start with the geodesic equation for a photon, which can be written as:

$$g_{\sigma\rho}\,\frac{dx^\rho}{d\lambda} \;=\; \frac{1}{2}\int d\lambda\;\frac{\partial g_{\mu\nu}}{\partial x^\sigma}\frac{dx^\mu}{d\lambda}\frac{dx^\nu}{d\lambda} \tag{2.1}$$

where λ is the affine parameter along the photon trajectory. The energy measured by an observer with four-velocity $u^\sigma = ((g_{tt})^{-1/2},0,0,0)$ is then

$$u^\sigma g_{\sigma\rho}\frac{dx^\rho}{d\lambda} = \frac{1}{2\sqrt{g_{tt}}}\int d\lambda\frac{\partial g_{\mu\nu}}{\partial t}\frac{dx^\mu}{d\lambda}\frac{dx^\nu}{d\lambda} \tag{2.2}$$

For a metric of the form $g_{\mu\nu} = a^2(\eta_{\mu\nu} + h_{\mu\nu})$ the change in the redshift with respect to the background $a^2\eta_{\mu\nu}$ to first order in the perturbations $h_{\mu\nu}$ is

$$\frac{\delta E}{E} = -\frac{1}{2}h_{tt} + \frac{1}{2}\int dt\;\frac{\partial h_{\mu\nu}}{\partial t}\gamma^\mu\gamma^\nu \tag{2.3}$$

where the integral is evaluated along the unperturbed geodesics

$$\frac{dx^\mu_{(0)}}{dt} = \gamma^\mu \tag{2.4}$$

with the direction cosines γ^μ. The redshift formula (2.3) agrees with the Sachs-Wolfe formula[4] for their choice of gauge condition.

Since the gravitational effects of a wall are limited by the horizon at the time t_* when the photon passes the wall we limit the range of integration in (2.3) to

$$|t - t_*| \leq (\frac{1}{a}\frac{\partial a}{\partial t})^{-1} \tag{2.5}$$

where $a/\partial_t a$ is the cosmic expansion scale that also determines the region of validity of the adiabatic approximation. We then get for the lower and upper limits of integration in (2.3) $t_1 = 2t_*/3$ and $t_2 = 2t_*$. In case that $2t_* > t_0$ we take $t_2 = t_0$:

$$t_1 = 2t_*/3 \quad , \quad t_2 = \min\{t_0, 2t_*\} \tag{2.6}$$

Formula (2.3) integrated between these limits constitutes the general redshift distortion formula which we will evaluate in the following paragraphs for perturbations $h_{\mu\nu}$ created by planar and spherical domain walls. In particular, we are interested in the dependence of $\delta E/E$ on the different parameters characterizing the wall.

3. Thick planar walls

In this paragraph we analyze the redshift distortion of photons in the gravitational field of thick planar walls in dependence of the scalar field potential $V(\Phi)$, the angle θ of the photon relative to the wall and the expansion rate H. We determine the metric in the weak field approximation for a scalar field with Φ^4- and sine-Gordon potentials. The expansion of the universe is taken into account in the adiabatic approximation.

Planar domain walls are scalar field configurations for which the energy density is concentrated in a sheet-like region and the scalar field $\Phi(t, z)$ attains different vacuum states on the different sides of the plane. In a matter dominated Friedman universe with metric $g_{\mu\nu} = a^2\ \eta_{\mu\nu}$ domain walls are described by solutions of the scalar field equation

$$\ddot{\Phi} - \Phi'' + 2\frac{\dot{a}}{a}\dot{\Phi} + a^2 V'(\Phi) = 0 \ , \tag{3.1}$$

with the boundary condition that Φ tends to two different minima of the scalar field potential $V(\Phi)$ as $z \to \pm\infty$. In this section we study the redshift distortion produced by planar domain walls for two different scalar field potentials: The

usual Φ^4-potential and the sine-Gordon potential (SG) which arises from the particle physics models discussed in Ref. 2:

$$V(\Phi) = \begin{cases} V_0 \left(1 - \dfrac{\Phi^2}{\Phi_0^2}\right)^2 \\ V_0 \cos^2\left(\dfrac{\pi\Phi}{2\Phi_0}\right) \end{cases} \tag{3.2}$$

with minima at $\Phi = \pm\Phi_0$. The solutions of the scalar field equation (3.1) describing a thick planar wall in the adiabatic approximation (where terms of $\dot{a}^2$ and $\ddot{a}$ are neglected) for the two potentials are:

$$\Phi(t,z) = \begin{cases} \Phi_0 \tanh(az/\delta) & \text{for } \Phi^4 \\ \Phi_0 \left[\dfrac{4}{\pi}\arctan\left(e^{az/\delta}\right) - 1\right] & \text{for SG} \end{cases}, \tag{3.3}$$

where δ is the wall thickness

$$\delta = \begin{cases} \dfrac{\Phi_0}{\sqrt{2V_0}} & \text{for } \Phi^4 \\ \sqrt{\dfrac{2}{V_0}}\dfrac{\Phi_0}{\pi} & \text{for SG} \end{cases}. \tag{3.4}$$

Note that the wall is localized in a region $|az| \leq \delta$, i.e. the proper thickness of the wall is not affected by the expansion. To determine the metric of the wall we also have to know the energy-momentum tensor for the adiabatic solutions (3.3):

$$\begin{aligned} T_t{}^t &= T_x{}^x = T_y{}^y = \rho \\ T_t{}^z &= -\frac{\dot{a}}{a} z\rho, \quad T_z{}^z = 0 \end{aligned} \tag{3.5}$$

where the energy density ρ is

$$\rho = \begin{cases} 2V_0/\cosh^4(az/\delta) & \text{for } \Phi^4 \\ 2V_0/\cosh^2(az/\delta) & \text{for SG} \end{cases} \tag{3.6}$$

Besides the thickness δ the other quantity that characterizes the wall phenomenologically is the surface density σ, which is defined by:

$$\sigma = \int_{-\infty}^{+\infty} d(az)\rho = \begin{cases} \dfrac{4}{3}\Phi_0^2/\delta & \text{for } \Phi^4 \\ \dfrac{8}{\pi^2}\Phi_0^2/\delta & \text{for SG} \end{cases} \tag{3.7}$$

In order to calculate the metric perturbations caused by the domain walls with energy momentum tensor (3.5) we make the following ansatz for the perturbed

metric

$$ds^2 = a^2(t)\Big[(1+h_{tt})dt^2 - (1-h_{zz})dz^2 - (1-h_{xx})(dx^2+dy^2)\Big] \ , \qquad (3.8)$$

where the metric perturbations $h_{\mu\nu}$ are functions of t and z. The linearized Einstein tensor in the adiabatic approximation for this Ansatz is

$$\begin{aligned} G_t{}^t &= \frac{1}{a^2} h''_{xx} \\ G_t{}^z &= -\frac{1}{a^2}\Big[\dot{h}'_{xx} - \frac{\dot{a}}{a} h'_{tt}\Big] \\ G_z{}^z &= 0 \\ G_x{}^x &= G_y{}^y = \frac{1}{2a^2}\Big[h''_{xx} - h''_{tt}\Big] \end{aligned} \qquad (3.9)$$

Note that the Einstein equations $G_{\mu\nu} = 8\pi G T_{\mu\nu}$ determine the solution only up to an arbitrary linear function of z. Usually the solution is uniquely determined by requiring that the $h_{\mu\nu}$ vanish far outside the source. Here, however, due to the one-dimensionality of the problem the gravitational field always diverges at large z. As we have shown[5] static planar walls do not admit Minkowski space on both sides, but create a Rindler- and Taub vacuum on the different sides of the wall. Demanding that the metric $\eta_{\mu\nu} + h_{\mu\nu}$ becomes Rindler space at $z \to +\infty$ and Taub-space at $z \to -\infty$ gives the following solution to the Einstein equations

$$\begin{aligned} h_{tt} &= -I - 2J \\ h_{zz} &= 3I \\ h_{xx} &= I - J \end{aligned} \qquad (3.10)$$

with

$$\begin{aligned} I &\equiv \begin{cases} 4\pi G\sigma\delta \ \big[\ln\cosh(az/\delta) - \cosh^{-2}(az/\delta)/4\big] & \text{for } \Phi^4 \\ 4\pi G\sigma\delta \ \ln\cosh(az/\delta) & \text{for SG} \end{cases} \\ J &\equiv 4\pi G\sigma a z \end{aligned} \qquad (3.11)$$

Note that although the $h_{\mu\nu}$ go linear with z at large $|z|$, the linear approximation remains valid within the horizon of the universe for all relevant choices of σ.

With the limits of integration given in (2.6) the redshift distortion for a planar wall is

$$\frac{\delta E}{E} = \frac{1}{2} I \Big|_{t_1}^{t_2} + J \Big|_{t_1}^{t_2} + \cos^2\theta \int_{t_1}^{t_2} dt \frac{\partial I}{\partial t} - \frac{1}{2}(2 + \sin^2\theta) \int_{t_1}^{t_2} dt \frac{\partial J}{\partial t} \tag{3.12}$$

where the integrals have to be evaluated along the unperturbed photon path $z = \cos\theta(t - t_*)$. The final expression for the redshift distortion is then

$$\frac{\delta E}{E} = 8\pi G\sigma H_*^{-1} \left\{ \frac{1}{2}\eta^2 \cos\theta + \cos^3\theta \left(\frac{1}{3}\eta^3 - \frac{1}{2}\eta^2\right) + \right.$$

$$\left. + \frac{1}{4}\delta H_* \left[\ln\cosh\left[\xi_*\eta^2(\eta-1)\right] - \frac{\alpha}{4}\cosh^{-2}\left[\xi_*\eta^2(\eta-1)\right] \right] + \cos^3\theta \; F_\alpha \right\} \Big|_{\eta_1}^{\eta_2} \tag{3.13}$$

where $\eta \equiv t/t_*$ and with

$$F_\alpha \equiv \int_{\eta_1}^{\eta_2} d\eta \; \eta(\eta-1) \left[(\alpha+2)\tanh(\xi_*\eta^2(\eta-1)) - \alpha \; \tanh^3(\xi_*\eta^2(\eta-1)) \right]$$

Here $H_* = H_0(1+z_*)^{3/2}$ is the Hubble parameter at cosmic redshift $(1 + z_*)=a(t_0)/a(t_*)$ and

$$\xi_* \equiv \frac{2\cos\theta}{H_*\delta} \tag{3.14}$$

Formula (3.13) yields the redshift distortion for the sine-Gordon potential ($\alpha = 0$) and for the Φ^4-potential ($\alpha = 1$). The limits of integration are $\eta_1 = 2/3$ and $\eta_2 = 2$ if $t_0 > 2t_*$ and $\eta_2 = \sqrt{1+z_*}$ if $t_0 < 2t_*$.

3.1 Dependence on $V(\Phi)$

The redshift distortion (3.13) is plotted in Fig.1 as a function of $H_*\delta$ for $\cos\theta = 1$. (Fig. 1 holds for $t_0 > 2t_*$; for $t_0 < 2t_*$ the shape is the same, only the height of the step is smaller.) It is evident from this curve that for $\delta \lesssim H_*^{-1}$ and $\delta >> H_*^{-1}$, i.e. for a wall thickness smaller and much larger than the horizon, the redshift distortion is completely independent from the scalar field potential $V(\Phi)$. Even for $\delta \approx H_*^{-1}$ the difference in $\delta E/E$ for the two potentials is only about 10%.

3.2 Dependence on the wall thickness δ

The redshift distortion in the regions $\delta \lesssim H_*^{-1}$ and $\delta >> H_*^{-1}$ is not only independent from the potential $V(\Phi)$ but also independent from the wall thickness. This is plausible because the gravitational field outside the wall becomes identical to the gravitational field of an infinitely thin wall. In the case that the wall thickness is much larger than the horizon, $\delta E/E$ becomes constant because the potential inside the wall does not vary on horizon scales. For the type of domain walls considered in Ref. 2 where δ can be as large as a few Mpc and $z_* \approx 100$ we find for instance that $\delta H_* \lesssim 1$ which becomes $\delta << H_*^{-1}$ as the universe evolves. We thus see that even walls as thick as a few Mpc induce the same redshift distortion as thin walls. Since no models with $\delta \gtrsim H_*^{-1}$ have been proposed yet, we will therefore consider only the thin wall limit, i.e. $\delta H_* \lesssim 1$.

3.3 Dependence on θ

For $\delta \lesssim H_*^{-1}$ the redshift distortion (3.13) simplifies for both potentials to

$$\frac{\delta E}{E} = 8\pi G\sigma H_*^{-1} \left\{ \frac{1}{2}\eta^2 \cos\theta + \frac{1}{2} \mid \cos\theta \mid \eta^2 |\eta - 1| \right.$$

$$\left. + \cos^3\theta \, (\frac{1}{3}\eta^3 - \frac{1}{2}\eta^2) + 2|\cos\theta|^3 \int d\eta \, \eta|\eta - 1| \right\} \Bigg|_{\eta_1}^{\eta_2} \qquad (3.15)$$

The angular dependence of this redshift distortion is depicted in Fig.2 . As expected $\delta E/E$ is maximal for photons moving perpendicular to the wall ($|\cos\theta| = 1$). The asymmetry of $\delta E/E$ with respect to a change of the direction of the photon ($\cos\theta \rightarrow -\cos\theta$) is due to the asymmetry of the metric which asymptotically becomes Rindler and Taub space. To receive photons with $\cos\theta > 0$ ($\cos\theta < 0$) the observer must be located in the Rindler space (Taub space).

For $\cos\theta > 0$, a photon that is emitted in the region $z < 0$ and crosses the wall at $z = 0$ at an angle θ, will be received by the observer at $z > 0$ at an angle θ with respect to the z-axis, see Fig. 3. Therefore, the angular distribution of $\delta E/E$ is given by the part of the curve in Fig. 2 with $0 \leq \cos\theta \leq 1$. This is sketched in Fig. 3. For $\cos\theta < 0$ the angular distribution of $\delta E/E$ is determined in a similar way by the part of the curve in Fig. 2 with $-1 \leq \cos\theta \leq 0$. In this case the incident angle of the photons is $\pi - \theta$. For walls at high cosmic redshifts ($z_* \geq 3$) the observer always sees a blueshift in both cases $\cos\theta > 0$ and

$\cos\theta < 0$. The maximum value of the blueshift is $\delta E/E \approx 6.2 \times 8\pi G\sigma H_*^{-1}$ for $\cos\theta = +1$ and $\delta E/E \approx 1.1 \times 8\pi G\sigma H_*^{-1}$ for $\cos\theta = -1$. For walls at low cosmic redshifts $z_* \leq 3$ an observer on the Taub side could see a redshift $\delta E/E < 0$.

3.4 Dependence on H_*

As one can see from Figs. 1 and 2 $\delta E/E$ is of the order $8\pi G\sigma H_*^{-1}$ on all angular scales and for all δ. For $z_* \geq 3$ $\delta E/E$ has a cosmic redshift dependence of $H_*^{-1} \propto (1+z_*)^{-3/2}$. For $z_* < 3$ there is an additional dependence on the cosmic redshift introduced via the upper limit of integration $\eta_2 = t_0/t_* = \sqrt{1+z_*}$, resulting in a decrease of $\delta E/E$ as $z_* \to 0$. Therefore domain walls at about $z_* \approx 3$ create the largest distortion. Note that the particular value $z_* = 3$ arises from our limits of integration eq. (2.6).

3.5 Moving walls

In this section we study the redshift distortion by planar walls with nonzero velocities with respect to the observer. We consider the gravitational field of a moving wall as a perturbation of the flat background and take account of the expansion of the universe by identifying the spatial coordinate z with the comoving coordinate. That is, we use the Lorentz-boosted metric of a static wall in formula (2.3) and replace $\gamma(z-vt)$ by $a(t)\gamma(z-vt)$. This is an approximate treatment which we believe yields the correct qualitative results. The metric of a static wall is given by (3.10), (3.11). After a Lorentz-boost in the z-direction with velocity v we get for the metric of a moving wall

$$ds^2 = a^2(t)\left(\eta_{\mu\nu} + h^v_{\mu\nu}\right) dx^\mu dx^\nu \tag{3.16}$$

with

$$\begin{aligned} h^v_{tt} &= \gamma^2\left[(3v^2-1)I - 2J\right] \\ h^v_{tz} &= 2v\gamma^2[I-J] \\ h^v_{zz} &= \gamma^2[(3-v^2)I - 2v^2 J] \\ h^v_{xx} &= h^v_{yy} = I - J \end{aligned} \tag{3.17}$$

where I and J are given by (3.10) and (3.11) with az replaced by $a\gamma(z-vt)$. The redshift distortion is again given by (2.3) where the integral is evaluated along the unperturbed photon path $z = \cos\theta\ (t-t_*) + vt_*$ between the limits given in (2.6). t_* is the time when the photon passes the wall, which is then located

at $z = vt_*$. The formula for the redshift distortion caused by a moving wall is ($\eta \equiv t/t_*$)

$$\frac{\delta E}{E} = 8\pi G\sigma H_*^{-1}\gamma^3 \left\{ |\cos\theta - v| \left[\frac{1}{2}(1-3v^2)\eta^2|\eta-1| + (v+\cos\theta)^2 \int d\eta\, 2\eta|\eta-1|\right]\right.$$

$$-\mathrm{sgn}(\cos\theta - v)\, v\, (\cos\theta + v)^2 \int d\eta\, \eta^2 \mathrm{sgn}(\eta-1) + (\cos\theta - v)\, \eta^2(\eta-1)$$

$$\left. + \frac{1}{2}\left[(\cos\theta+v)^2 - 3(1+v\cos\theta)^2\right] \left[(\cos\theta - v)(\frac{2}{3}\eta^3 - \eta^2) - \frac{1}{3}\, v\, \eta^3\right]\right\}\Bigg|_{\eta_1}^{\eta_2} \quad (3.18)$$

with $\eta_1 = 2/3$ and $\eta_2 = \min\{2, \sqrt{1+z_*}\}$. This formula applies for the physically relevant case $\delta \lesssim H_*^{-1}$ and is shown in Fig. 4 as a function of v. For $v = 0$ this expression reduces to formula (3.15). A salient feature of this redshift distortion for moving walls is a velocity dependence that goes roughly as γ^3. This dependence is due to a γ^2 factor from the Lorentz-boosted energy momentum tensor of the wall and another γ factor from the linear $z-$dependence of the domain wall metric. Compared to the formula (3.15) another new feature for moving walls is the occurance of a redshift, i.e. $\delta E/E < 0$ for $\cos\theta < 0$. Note that photons with $\cos\theta > 0$ ($\cos\theta < 0$) can only be received by observers in the region $z > 0$ ($z < 0$). Also, for photons to actually pass the wall the following relations have to be satisfied:

$$\cos\theta > 0 \quad : \quad -1 < v < \cos\theta$$

$$\cos\theta < 0 \quad : \quad \cos\theta < v < 1$$

since for $v = \cos\theta$ the wall and the photon have the same velocity along the $z-$axis. Fig. 4 shows that in the case $\cos\theta > 0$ $\delta E/E$ is always positive, i.e. photons are blueshifted, whereas for $\cos\theta < 0$ $\delta E/E$ becomes negative for large velocities or low cosmic redshifts z_*.

3.6 UPPER BOUND ON σ

The observed isotropy of the microwave background imposes a constraint on the surface energy density σ. We found that the maximal distortion of the microwave background occurs for photons crossing a domain wall at a cosmic redshift $z_* \approx 3$. The magnitude of this distortion is $\delta E/E \approx 0.78 \times 8\pi G\sigma H_0^{-1}$, see Fig. 2. This has to be compared with the observational upper bound on the temperature fluctuations[6] $\delta T/T \lesssim 4 \times 10^{-5}$ (at angular scales $\lesssim 10°$). We therefore find for the upper bound on the surface energy density $\sigma \lesssim 0.6$ MeV^3.

Numerical simulations for a network of domain walls have shown[3] that the r.m.s. velocity of the walls is about 0.4. Since $\delta E/E$ is enhanced by a factor γ^3 for walls with $v \neq 0$ one could derive a stronger bound on σ using the expressions for the redshift distortion of high-velocity walls. However, such a bound would only be reliable if the exact velocity distribution of the network of domain walls were known.

4. Spherical walls

We first consider the redshift distortion for photons passing outside a spherical domain wall. Then we briefly discuss the case of photons traversing through the bubble. A detailed analysis of the angular patterns of distortion in the microwave background caused by collapsing spherical domain walls in Ref. 7 is based on this section.

Due to the spherical symmetry, the gravitational field outside the bubble is identical to that of a point mass. Therefore the gravitational field outside the bubble is independent from the dynamics of the bubble. As an ansatz for the metric of the bubble in an expanding universe we take

$$ds^2 = a^2(t)\left[(1+h_{tt})dt^2 - (1-h_{rr})dr^2 - r^2\, d\Omega^2\right] \tag{4.1}$$

The linearized vacuum Einstein equations in the adiabatic approximation (terms with $\dot{a}^2, \ddot{a}$ are neglected) are :

$$\begin{aligned} h'_{rr}r + h_{rr} &= 0 \\ h'_{tt}r + h_{rr} &= 0 \\ \dot{a}\, h_{tt}r - a\dot{h}_{rr} &= 0 \end{aligned} \tag{4.2}$$

The solution of these equations is

$$h_{tt} = h_{rr} = -\frac{2GM}{ar} \tag{4.3}$$

where M is the mass of the bubble. This solution has to be inserted into the general redshift formula (2.3). The integral is then evaluated along the unperturbed photon path $r(t) = \sqrt{(t-t_*)^2 + r_*^2}$ where t_* is the time when the photon passes the bubble at a distance r_*. With the same limits of integration as in section 2, $t_1 = 2t_*/3$, $t_2 = \min\{2t_*, t_0\}$, and with the abbreviations $\beta \equiv r_*/t_*$, $\eta \equiv t/t_*$ we obtain:

$$\frac{\delta E}{E} = 2GMH_* \left\{ \frac{\beta^4 - 10\beta^2 + 4}{4(\beta^2+1)^{7/2}} \operatorname{asinh}\Big(\frac{\eta - \beta^2 - 1}{|\beta|\,|\eta|}\Big) + \right.$$

$$\left. + \frac{\eta^3(7\beta^2 - 8) + \eta^2(12 - 17\beta^2 + \beta^4) - \eta(1+\beta^2)(2-3\beta^2) - (1+\beta^2)^2}{4\eta^2(1+\beta^2)^3\left[\beta^2 + (\eta-1)^2\right]^{1/2}} \right\} \Bigg|_{\eta_1}^{\eta_2} \tag{4.4}$$

β is the ratio of the proper distance $l_* = a(t_*)r_*$ corresponding to r_* and the horizon size $2H_*^{-1}$: $2\beta = l_*H_*$. In Fig. 5 we give the redshift distortion (4.4) for a photon passing outside a bubble as a function of l_*H_*. As expected, for $l_* \approx H_*^{-1}$, i.e. for an impact parameter of the order of the horizon, the photon is not affected by the gravitational field of the bubble, so that $\delta E/E$ vanishes. For $l_* < H_*^{-1}$ $\delta E/E$ shows a logarithmic dependence which can be obtained from (4.4) in the limit $\beta \to 0$:

$$\frac{\delta E}{E} = 4GMH_* \left\{ \ln\big(2/(l_*H_*)\big) - \frac{19}{16} \right\} \quad (\text{for } \beta \to 0) \tag{4.5}$$

Note that l_* is always larger than the Schwarzschild radius $\mathcal{R} = 2GM$ which means that there is a maximal value of $\delta E/E$. The result (4.5) can also be derived by a qualitative analysis similar to the one used by Rees and Sciama[8] for the redshift distortion created by density inhomogeneities separating out from the Hubble expansion. The dominant effects contributing to the redshift distortion of a photon passing a point mass are the time delay caused by the gravitational potential and the change of the gravitational field due to the background expansion. The time delay for a photon in the potential of a point mass is

$$\Delta t \approx 2\int_{r_*}^{t_*} dr(1 - \frac{2M}{r})^{-1} - 2t_* = 4GM\ln\big(2/(l_*H_*)\big)$$

yielding a contribution to the redshift $\delta E/E = H_*\Delta t$ which is exactly the first

term in (4.5). The contribution due to the change of the gravitational field is

$$\approx -\frac{1}{2}h_{tt}\Big|_{2t_*/3}^{2t_*} = -4GMH_*(\frac{13}{16})$$

This approximates the second term in (4.5). The blueshift from the time delay always exceeds the redshift from the changing gravitational field so that the photon achieves a net gain of energy.

Photons that traverse the collapsing bubble experience no gravitational field while they are inside the bubble. Before entering and after leaving the bubble they see a Schwarzschild field (4.3). The main contribution to the redshift distortion for these photons comes from the difference in the gravitational potential when they enter and leave the bubble. Since the bubble collapses the photon leaves the bubble at a radius $r_{\rm out}$ which is much smaller than the radius when the photon enters the bubble. The redshift distortion is therefore approximately

$$\frac{\delta E}{E} \approx -\frac{1}{2}h_{tt} \approx -GM/(a(t_{\rm out})r_{\rm out}) \ . \tag{4.6}$$

This leads to red spikes in the microwave background whereas the photon that passes only outside the bubble at larger impact parameters r_* receives a blueshift, as was shown above. The overall pattern of redshift distortion produced by collapsing spherical domain walls consists therefore of red spikes surrounded by blue discs.

So far, we implicitly assumed that the final state of the bubble collapse is a black hole. There is, however, the possibility that the bubble evaporates into Φ-bosons as it shrinks to a radius equal to the inverse boson mass[9] . Since the emitted bosons form an expanding shell with vanishing gravitational field inside and Schwarzschild field outside, the pattern of the redshift distortion is a blue spike surrounded by a blue disc, analogous to the case of the collapsing bubble discussed above. This pattern was analyzed in detail in Ref. 7. The red and blue spikes surrounded by blue discs form a characteristic redshift pattern that can serve as an unambiguous indicator for collapsing domain walls. This is because the width and the height of a spike is related to the diameter and magnitude of the surrounding blue disc[7] . The largest redshift distortion in discs occurs for low cosmic redshifts since the mass of a bubble that begins to collapse at about $t_0/2$ is given by $M = 4\pi G\sigma H_0^{-2}/16$:

$$\frac{\delta E}{E}\Big|_{\rm disc} \approx \pi G\sigma H_0^{-1} \ . \tag{4.7}$$

The largest redshift distortion in spikes eq. (4.6) occurs for small $r_{\rm out}$, i.e. the

collapsing bubble must be close to our past light cone:

$$\left.\frac{\delta E}{E}\right|_{\text{spike}} \approx \frac{\pi G\sigma H_*^{-2}}{4l_{\text{out}}} \tag{4.8}$$

with $l_{\text{out}} = a(t_{\text{out}})r_{\text{out}}$. Spikes produce the largest signals, $\delta E/E|_{\text{spike}} > \delta E/E|_{\text{disc}}$ for

$$l_{\text{out}}H_* < H_0/(4H_*) \ , \tag{4.9}$$

i.e. spikes at large cosmic redshifts exceed the discs at low cosmic redshifts if the radius l_{out} is much smaller than the horizon. One therefore expects that the number of spikes of this magnitude is only a small fraction of the total number of spikes. The total number of spikes is readily obtained by integrating the number density of collapsing bubbles[3] $dN/(dt_*\, d^3r_*) = t_*^{-4}$ over a horizon volume around our past light cone, i.e. $|(t_0 - t_*) - r_*| \lesssim t_*$ and $t_{\text{ls}} < t_* < t_0$, where t_{ls} is the epoch of the last scattering of the MBR-photons. One finds $N_{\text{tot}} \lesssim 4\pi(1 + z_{\text{ls}})$. The number of spikes exceeding the blue discs at low redshift is much smaller than N_{tot} since they occur only if a bubble collapses very close to our past light cone: $|(t_0 - t_*) - r_*| \lesssim r_{\text{out}} \lesssim t_*^4/(8t_0^3)$, see eq. (4.9). In this case one finds $dN/dt_* \approx \pi(t_0 - t_*)^2/t_0^3$ which gives $N \approx 1$, showing that those spikes are very rare. The resulting redshift pattern in the MBR sky produced by collapsing domain walls therefore is dominated by a few blue discs of amplitude (4.7). At smaller values of $\delta E/E$ a characteristic pattern of blue and red spikes surrounded by blue discs appears that can be an unique signal from collapsing domain walls.

5. Summary

We have analyzed the redshift distortion by planar and spherical domain walls. For both of these topologically different configurations we found that $\delta E/E$ is generally of the order $\pi G\sigma H_*^{-1}$. Therefore, domain walls at lower cosmic redshifts create the largest distortions. Also, $\delta E/E$ is independent of the wall thickness δ and the form of the scalar field potential $V(\Phi)$ if δ is smaller than the horizon at the time when the photon passes the wall. The angular pattern of the redshift distortion imprinted on the MBR sky was outlined in sections 3 and 4 for planar and spherical walls. The most prominent distortions occur on scales that are currently measured by the COBE-satellite. COBE can detect redshift distortions that would arise from models with σ smaller than the upper bound derived in this paper, $\sigma \lesssim 1$ MeV^3. An example for such a model is the late time phase transition scenario by Hill, Schramm and Fry[2] .

6. Acknowledgements

We thank Dave Schramm for drawing our attention to this subject. This work was supported by NSF AST88-22595 and NASA-NAGW-1321 at Chicago, by NASA-NAGW-1340 at Fermilab and by a Feodor-Lynen-fellowship of the Alexander-von-Humboldt foundation (G.G.).

REFERENCES

1. Ya. Zeldovich, I.Yu. Kobzarev and L.B. Okun, *Zh. Eksp. Teor. Fiz.* **67** (1974) 3 [*Sov. Phys. JETP* **40** (1975) 1].
2. Ch.T. Hill, D.N. Schramm and J. Fry, *Com. Nucl. Part. Phys.* **19** (1989) 25; Ch.T. Hill, D.N. Schramm and L.M. Widrow, Fermilab-Pub-89/166-T, preprint, 1989.
3. W.H. Press, B.S. Ryden and D.N. Spergel, *Astrophys. J.* **347** (1989) 590.
4. R.K. Sachs and A.M. Wolfe, *Astrophys. J.* **147** (1967) 73.
5. G. Goetz and D. Nötzold, Fermilab-Pub-89/236-A, preprint Oct. 1989.
6. R.D. Davies et al., *Nature* **326** (1987) 462.
7. G. Goetz and D. Nötzold, Fermilab-Pub-90/149-A, preprint July 1990.
8. M.J. Rees and D.W. Sciama, *Nature* **217** (1968) 511.
9. L.M. Widrow, *Phys. Rev.* **D40** (1989) 1002.

FIGURE CAPTIONS

1. Redshift distortion caused by a planar wall as a function of δH_* for the two scalar field potentials.
2. Redshift distortion caused by a planar wall as a function of the angle θ for different cosmic redshifts z_*.
3. Sketch of the angular pattern of the redshift distortion caused by a planar wall.
4. Redshift distortion as a function of the velocity v of a planar wall for different angles θ: (a) $z_* \geq 3$, (b) $z_* = 0.5$.
5. Redshift distortion as a function of the impact parameter β for a photon passing outside a spherical wall.

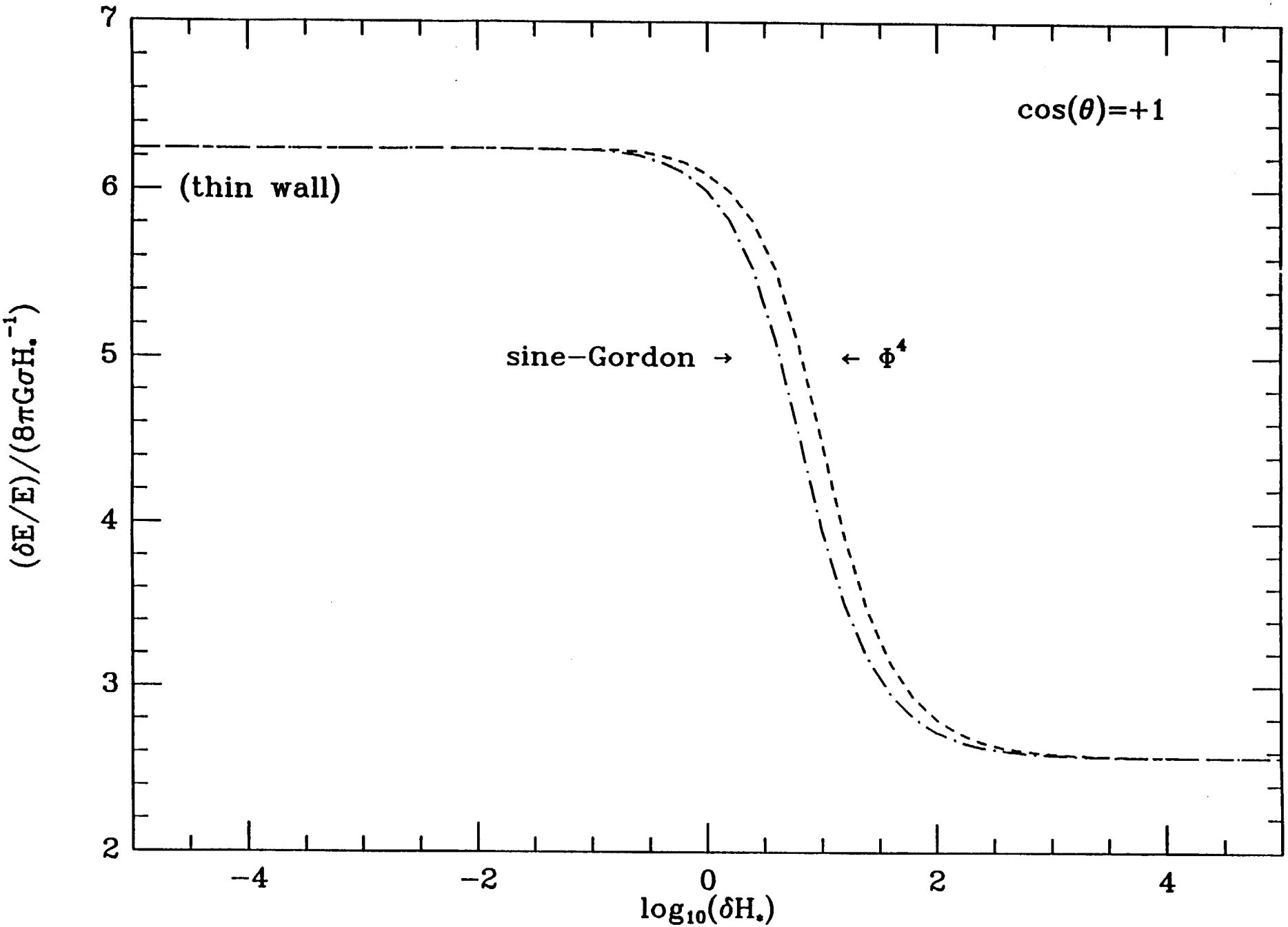
cos(θ)=+1
(thin wall)
sine−Gordon →
← Φ⁴
(δE/E)/(8πGσH*⁻¹)
log₁₀(δH*)
7
6
5
4
3
2
−4
−2
0
2
4

Fig. 1

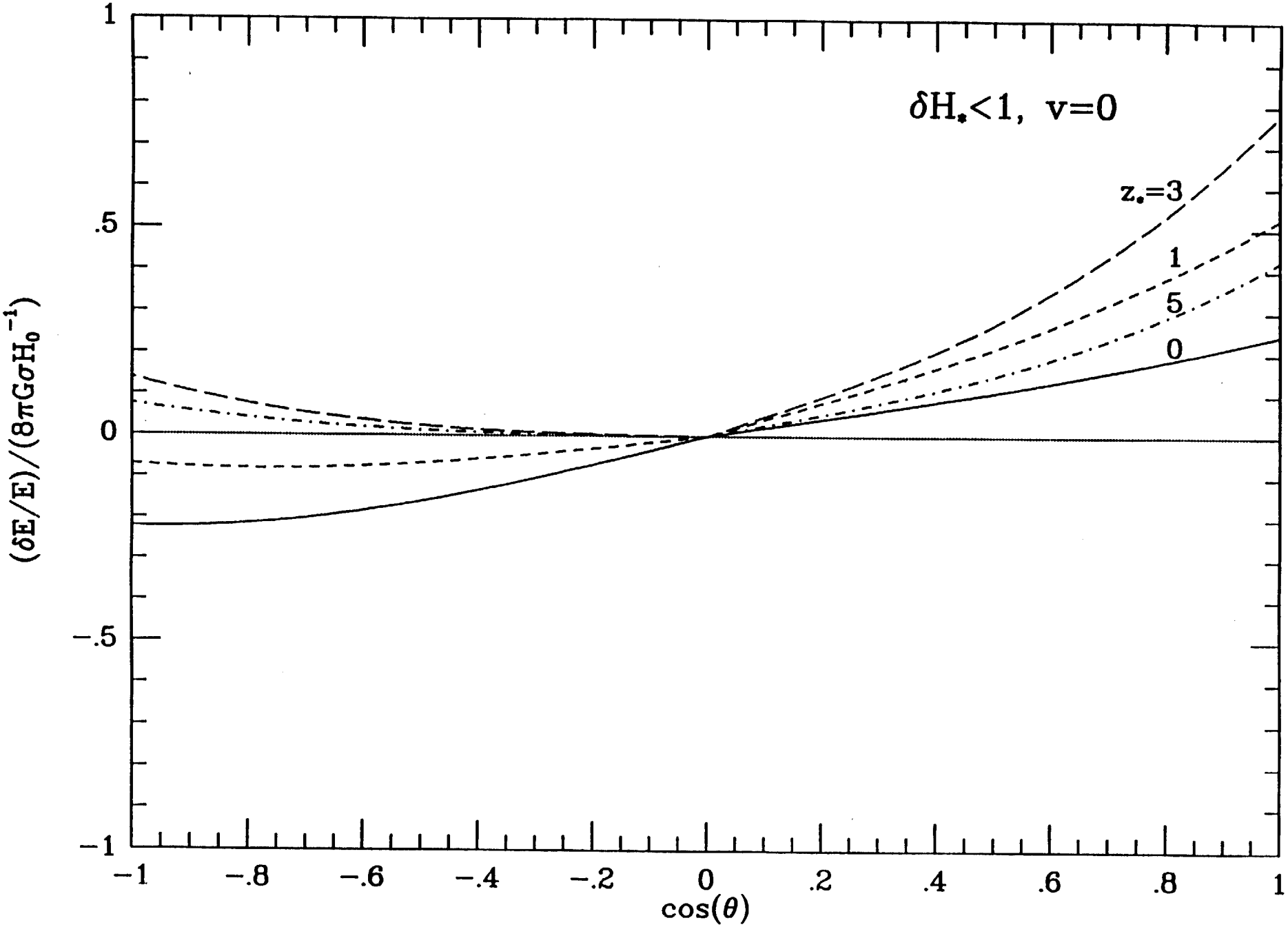

Fig. 2

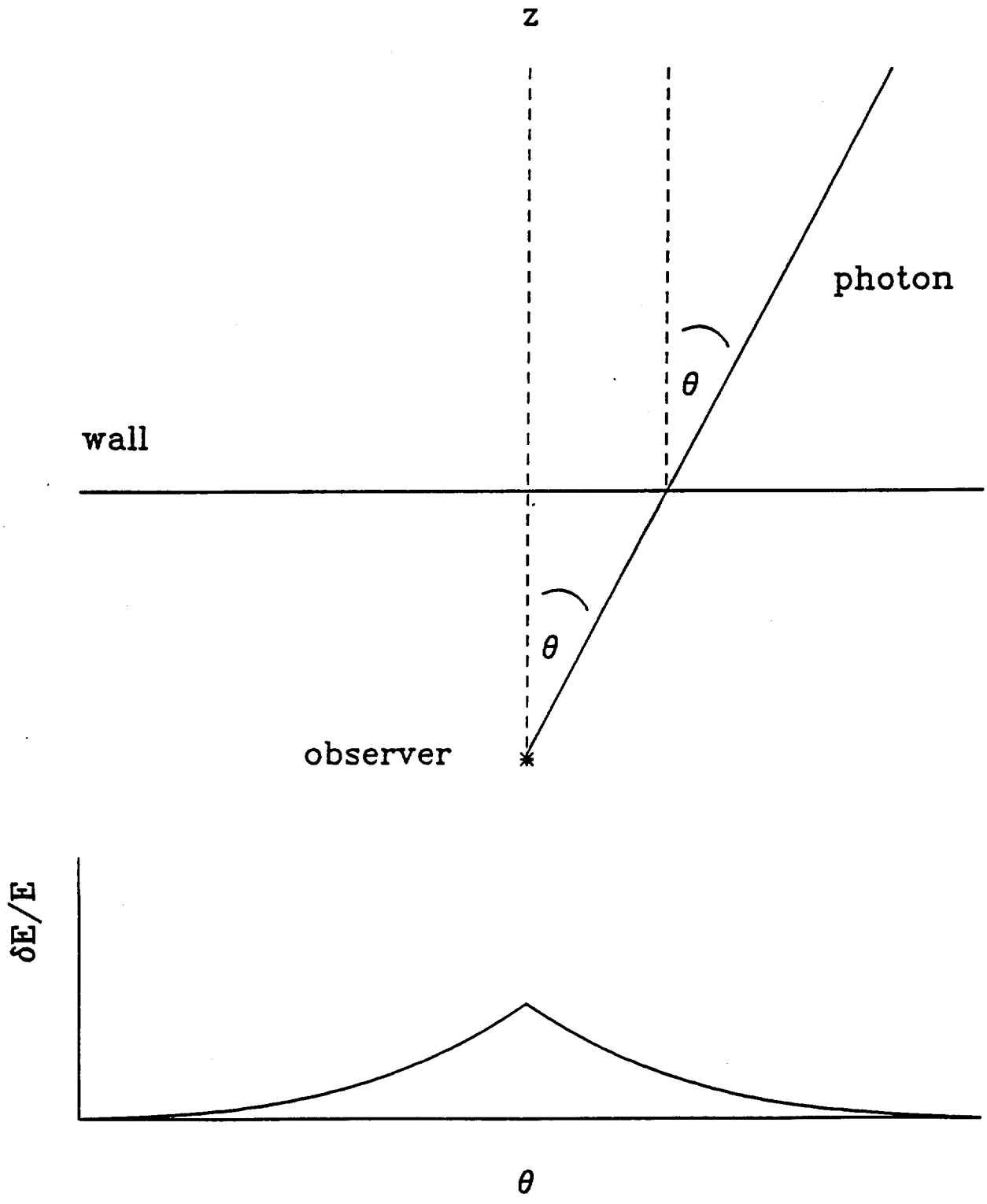

Fig. 3

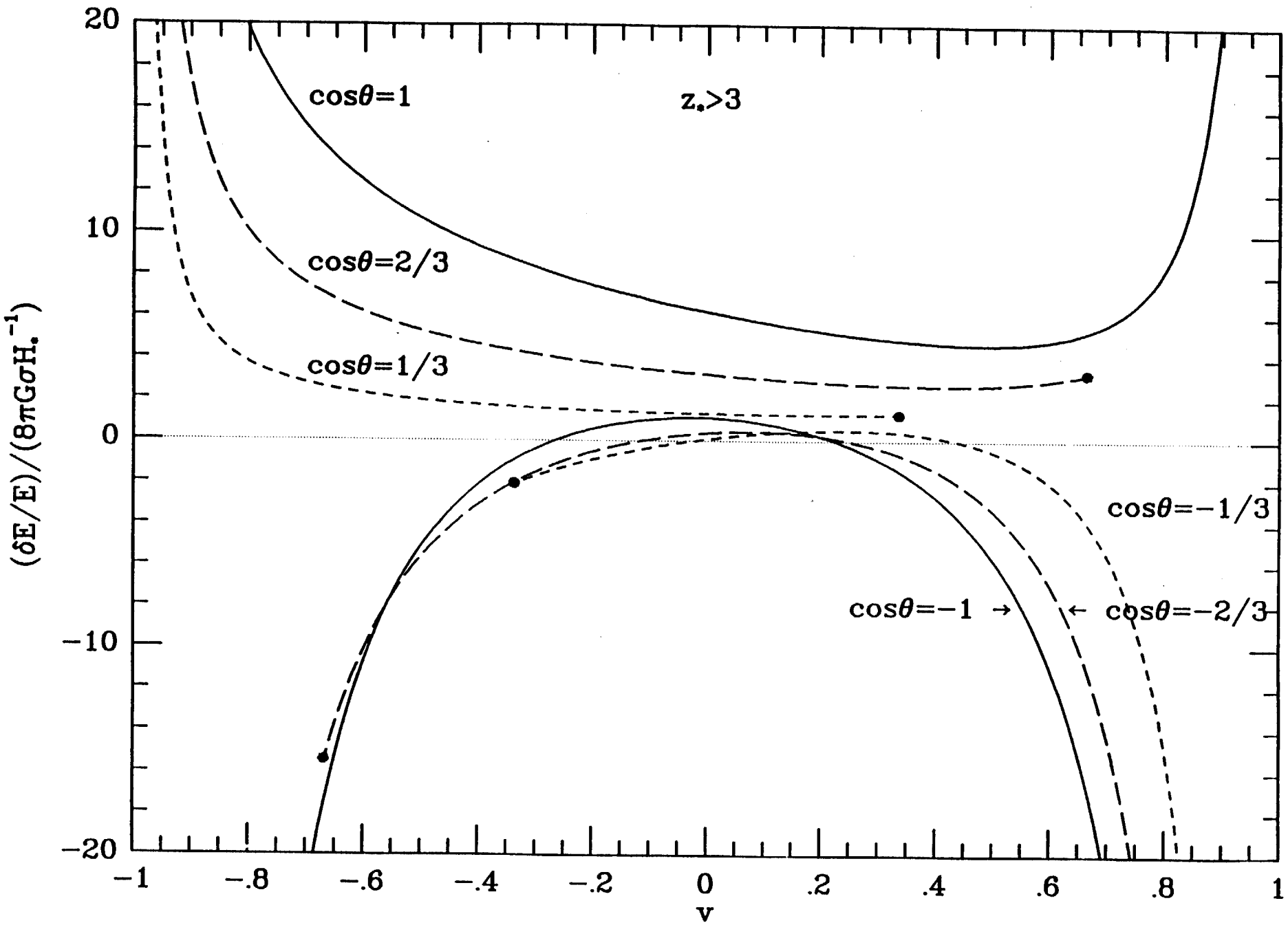
20
10
0
−10
−20
−1
−.8
−.6
−.4
−.2
0
.2
.4
.6
.8
1
v
(δE/E)/(8πGσH*⁻¹)
cosθ=1
z*>3
cosθ=2/3
cosθ=1/3
cosθ=−1/3
cosθ=−1 →
← cosθ=−2/3

Fig. 4a

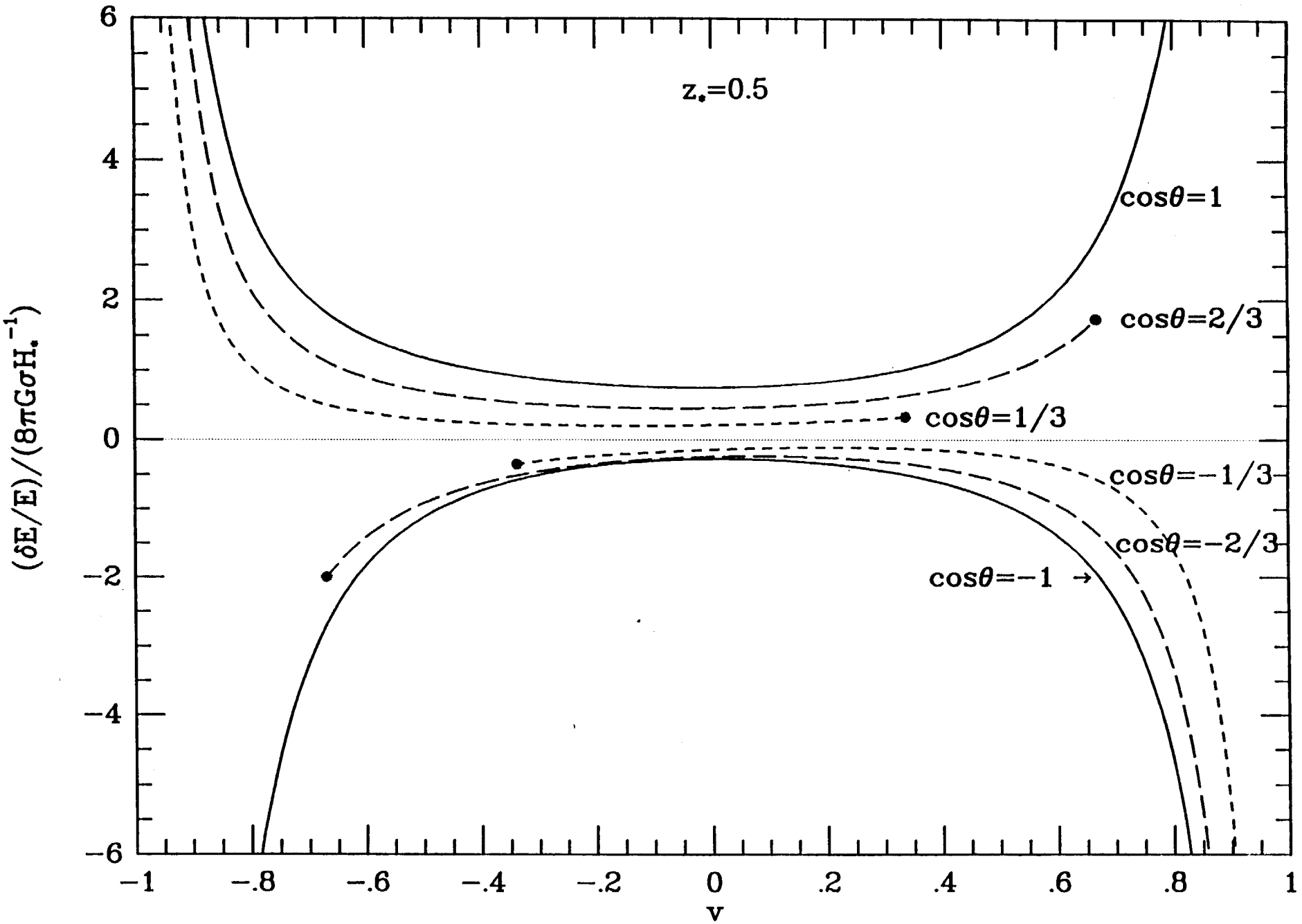
z*=0.5
cosθ=1
cosθ=2/3
cosθ=1/3
cosθ=−1/3
cosθ=−2/3
cosθ=−1
(δE/E)/(8πGσH*^-1)
v
6
4
2
0
−2
−4
−6
−1
−.8
−.6
−.4
−.2
0
.2
.4
.6
.8
1

Fig. 4b

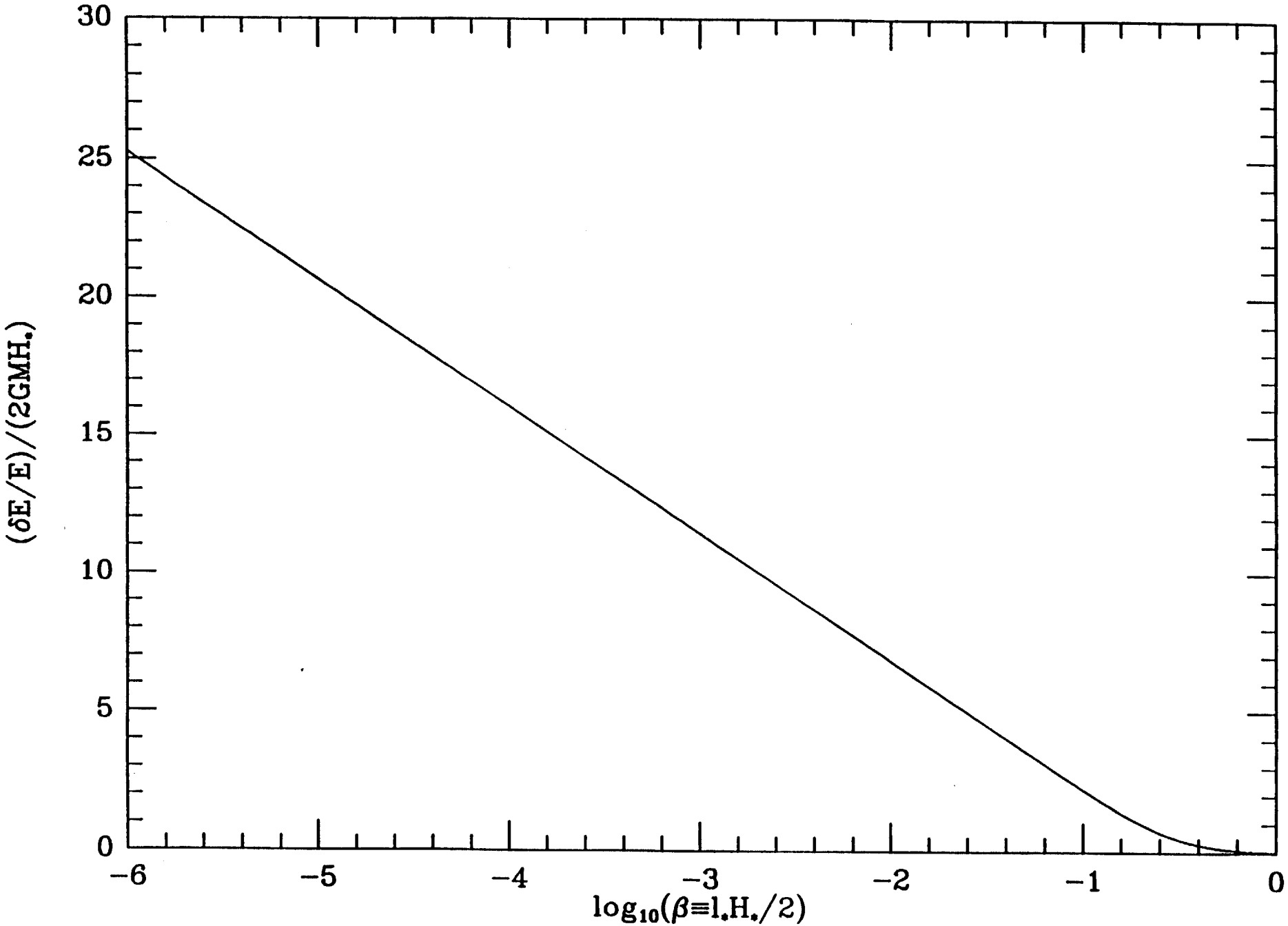

Fig. 5